TECHNICAL REPORT AMR-SS-08-10

THE AERODYNAMIC INFLUENCE OF A HELICOPTER ON A JETTISONED MISSILE

Milton E. Vaughn, Jr.
System Simulation and Development Directorate
Aviation and Missile Research, Development, and Engineering Center

January 2008

DESTRUCTION NOTICE

FOR CLASSIFIED DOCUMENTS, FOLLOW THE PROCEDURES IN DoD 5200.22-M, INDUSTRIAL SECURITY MANUAL, SECTION II-19 OR DoD 5200.1-R, INFORMATION SECURITY PROGRAM REGULATION, CHAPTER IX. FOR UNCLASSIFIED, LIMITED DOCUMENTS, DESTROY BY ANY METHOD THAT WILL PREVENT DISCLOSURE OF CONTENTS OR RECONSTRUCTION OF THE DOCUMENT.

DISCLAIMER

THE FINDINGS IN THIS REPORT ARE NOT TO BE CONSTRUED AS AN OFFICIAL DEPARTMENT OF THE ARMY POSITION UNLESS SO DESIGNATED BY OTHER AUTHORIZED DOCUMENTS.

TRADE NAMES

USE OF TRADE NAMES OR MANUFACTURERS IN THIS REPORT DOES NOT CONSTITUTE AN OFFICIAL ENDORSEMENT OR APPROVAL OF THE USE OF SUCH COMMERCIAL HARDWARE OR SOFTWARE.

REPORT DOCUMENTATION PAGE

Form Approved
OMB No. 074-0188

1. AGENCY USE ONLY	2. REPORT DATE	3. REPORT TYPE AND DATES COVERED
	January 2008	Final

4. TITLE AND SUBTITLE
The Aerodynamic Influence of a Helicopter on a Jettisoned Missile

5. FUNDING NUMBERS

6. AUTHOR(S)
Milton E. Vaughn, Jr.

7. PERFORMING ORGANIZATION NAME(S) AND ADDRESS(ES)
Commander, U.S. Army Research, Development, and Engineering Command
ATTN: AMSRD-AMR-SS-AT
Redstone Arsenal, AL 35898

8. PERFORMING ORGANIZATION REPORT NUMBER
TR-AMR-SS-08-10

9. SPONSORING / MONITORING AGENCY NAME(S) AND ADDRESS(ES)

10. SPONSORING / MONITORING AGENCY REPORT NUMBER

11. SUPPLEMENTARY NOTES

12a. DISTRIBUTION / AVAILABILITY STATEMENT
Approved for Public Release; distribution is unlimited.

12b. DISTRIBUTION CODE
A

13. ABSTRACT *(Maximum 200 Words)*

The effect of the presence of a helicopter fuselage on the aerodynamic behavior of an unthrusted, jettisoned missile with forward strakes and tail control surfaces is explored. The investigative tool used for this purpose is a production-oriented, Euler, Computational Fluid Dynamics (CFD) methodology Titled Euler Tunnel Analysis (ETA). Initially, comparison of CFD computations with wind tunnel measurements for the isolated missile are used to anchor the computations in reality and provide an evaluation benchmark. The ensuing study is assumed to be sufficiently fast so as to convect rotor downwash effects downstream of the region of interest. Further, the calculations are performed in steady-state mode for each scenario. As expected, it is found that even without downwash the presence of the fuselage significantly modifies the aerodynamic properties of the missile. In addition, the vorticity confinement method (which conserves field and surface vorticity) is shown to preserve the vorticity created by the forward strakes as it convects downstream to the tail controls.

14. SUBJECT TERMS	15. NUMBER OF PAGES
Helicopter, Aerodynamic Influence, Missile with Strakes, Computational Fluid Dynamics, Aerodynamic Design	32
	16. PRICE CODE

17. SECURITY CLASSIFICATION OF REPORT	18. SECURITY CLASSIFICATION OF THIS PAGE	19. SECURITY CLASSIFICATION OF ABSTRACT	20. LIMITATION OF ABSTRACT
UNCLASSIFIED	UNCLASSIFIED	UNCLASSIFIED	SAR

NSN 7540-01-280-5500

Standard Form 298 (Rev. 2-89)
Prescribed by ANSI Std. Z39-18
298-102

ACKNOWLEDGMENTS

This work was supported in part by a grant of High Performance Computer (HPC) time from the Naval Oceanographi (NAVO) Department of Defense (DOD) HPC center on their Cray-SV1.

TABLE OF CONTENTS

LIST OF ILLUSTRATIONS

I. INTRODUCTION

The static stability of a missile with forward strakes and tail controls (Fig. 1) is typically dominated by the influence of strake-generated vortices on the tail at small to moderate angles of attack. Consequently, when such missiles are to be integrated with a helicopter launch platform, the effect of the helicopter on the vortical interactions must be taken into account. While this is important to the correct modeling of flight performance during launch, it is critical to accurately assessing the missile trajectory during an emergency jettison event. A collision between the missile and the helicopter could be catastrophic.

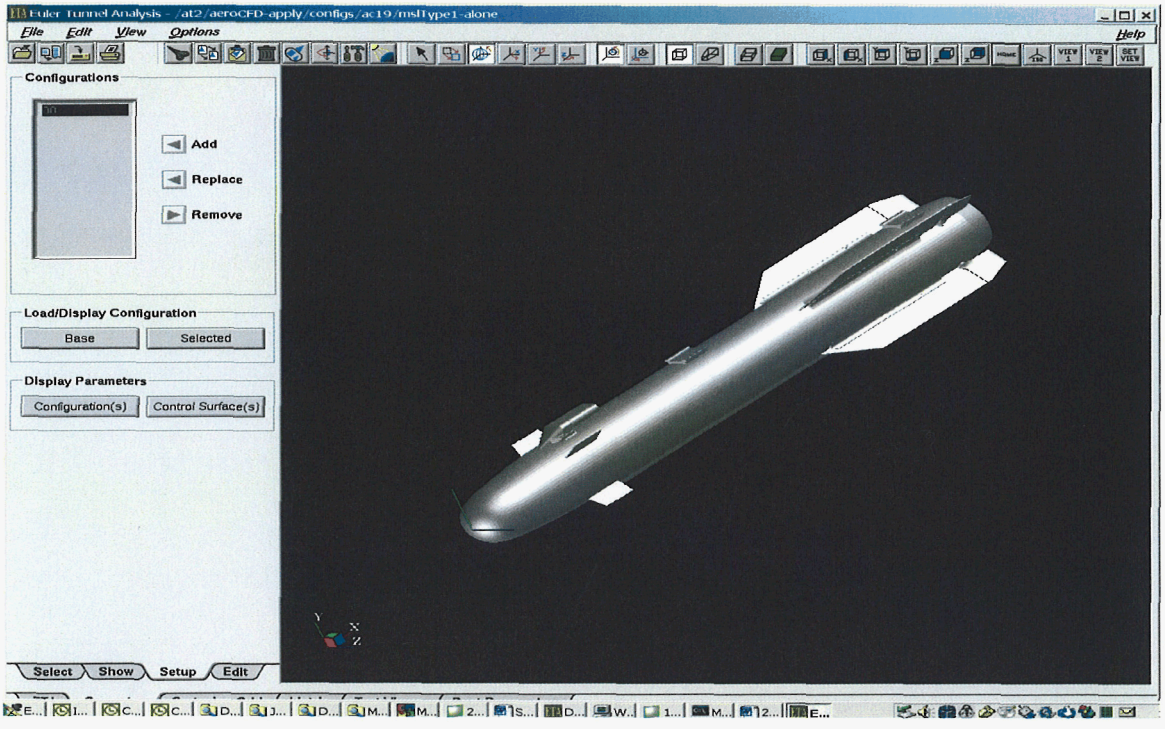

Figure 1. Overall View of Missile with Forward Strakes and Tail Controls

To determine appropriate jettison procedures, it is vital that numerous trajectory simulations be performed before conducting full-scale hardware tests which are very expensive. However, high quality aerodynamic data is needed to predict realistic flight paths. Wind tunnel measurements can readily provide high quality, cost-effective aerodynamics for an isolated missile. However, tunnel testing of actual helicopter/missile jettison configurations is quite expensive due to the large number of geometric possibilities. To provide the required aerodynamic data, one could apply any of several well-established, viscous, overset Computational Fluid Dynamics (CFD) methods. Unfortunately, numerous aerodynamic scenarios must be calculated to provide sufficient data for simulation purposes. The substantial amount of time required to create appropriate solution grids, properly exercise the solver, analyze the results, and extract aerodynamic coefficients prevents these approaches from providing timely input to such problems.

It is worth noting, though, that helicopters usually release missile stores from external wings or open bay doors (Fig. 2), as opposed to an interior weapons bay. Further, the flight speeds

involved are typically too slow for an unthrusted missile to generate substantial lift. For example, the airframe shown in Figure 1 would only generate a lift force equal to approximately 3 percent of its weight at a velocity of 120 knots and a 2 degree angle of attack. As a result, jettisoned stores drop quickly from near-field, viscous flow into predominantly inviscid flow. The principal effects on the missile are thus volumetric, rotational, and vortical disturbances created by the helicopter. This type of environment can be properly addressed in a timely and cost-effective manner by means of a responsive, Euler CFD method.

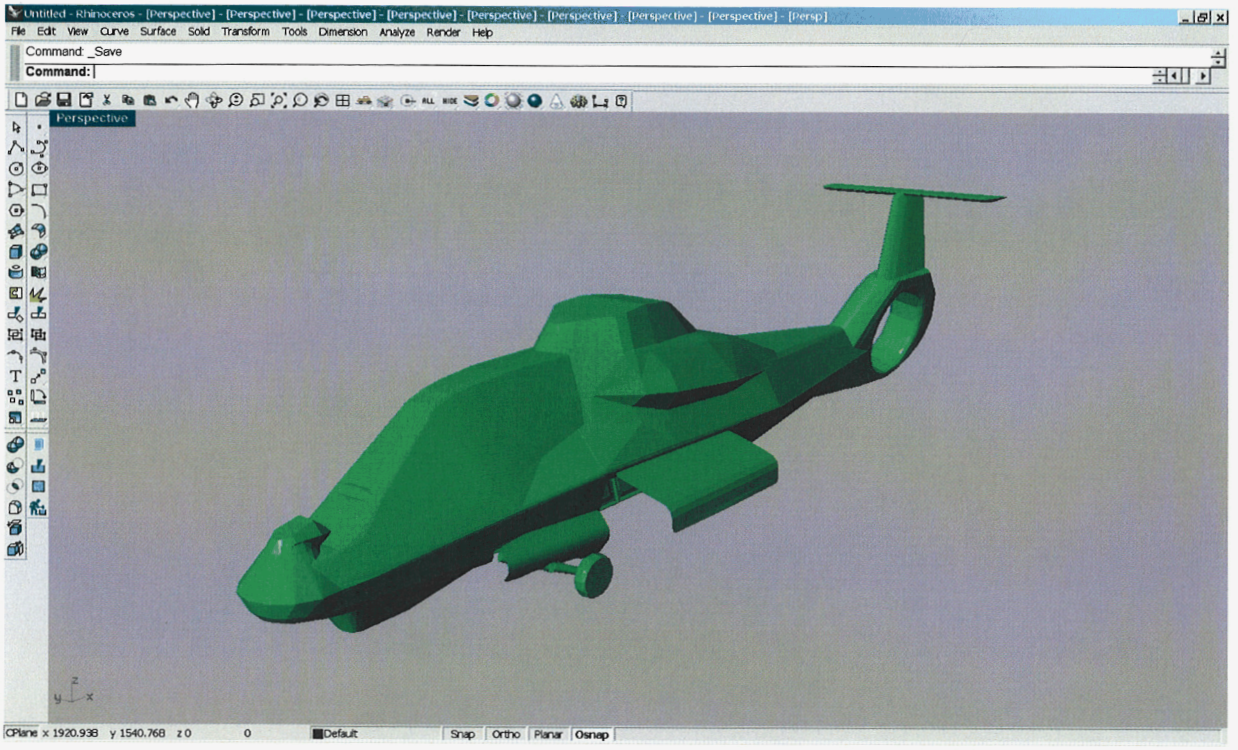

Figure 2. Overall View of Helicopter with Bay Doors Open

Such a method exists and is called the Euler Tunnel Analysis (ETA) methodology. ETA is a productivity-oriented system of CFD software that is designed to enable the use of CFD without specialized computational expertise. ETA uses the NASA/Ames **Cart**esian 3D (Cart3D) methodology [1] to create unstructured, hexahedral solution grids in an automated fashion, and it applies the NASA/Ames Topology Independent Gridding Euler Refinement (TIGER) solver [2] (as modified by Robinson [3,4]) to compute the flowfield. A Graphical User Interface (GUI) and several software scripts are employed to enable: (1) editing of body geometries, (2) generation of the solution grid, (3) establishment of aerodynamic points of interest (that is, Mach numbers, angles of attack, roll angles, and control deflection angles) in a "point and click" fashion, (4) creation of the required directory structures and input files, (5) submission of cases to the computational platform, (6) checking the status of each case, (7) retrieval of the results, and (8) calculation of aerodynamic coefficients from each solution.

For the helicopter jettison problem, ETA was used to compute the effects of a detailed helicopter body (Figs. 2 and 3) on the aerodynamic properties of a missile with forward strakes (Fig. 1) at various potential trajectory points. The objective was not to simulate the missile

trajectory with time-accurate CFD, but rather to provide correct aerodynamic force and moment coefficients for use in a "faster-running" Six-Degree-of-Freedom (6-DOF) flight simulation. This 6-DOF currently uses freestream aerodynamic coefficients that vary with Mach number and body attitude but not position with respect to other bodies. Since the geometric possibilities are numerous, it was highly desirable to account for body proximity effects via corrections to the freestream coefficients of the isolated missile. This was a simpler and much more manageable tactic than constructing position-specific aerodynamic properties. It was with this in mind that ETA was exercised to investigate the extent and magnitude of helicopter effects on the jettisoned missile.

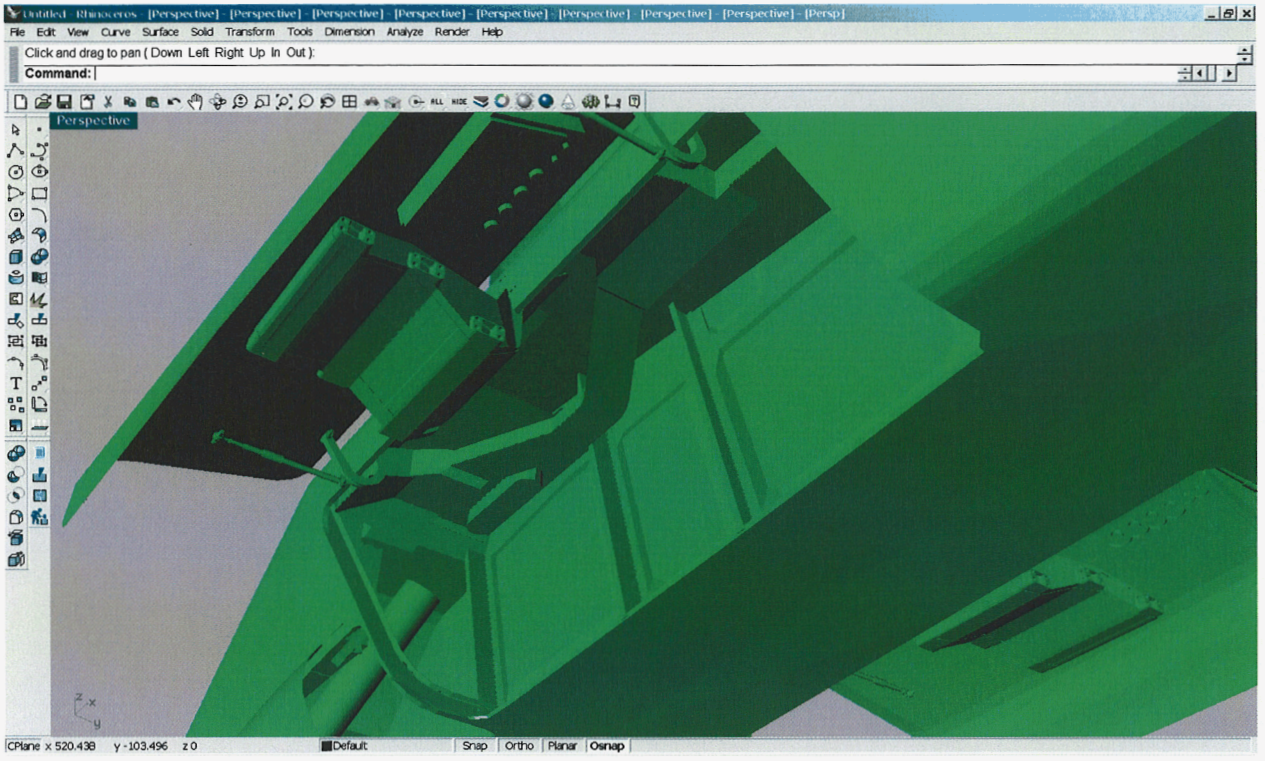

Figure 3. Close-Up of Weapons Bay (Viewed from Below Looking Forward)

II. METHODOLOGY

A. Description

ETA is a suite of Government-owned, productivity-oriented, CFD software developed to facilitate aerodynamic design and analysis. While it is described in Reference 5, it is important to make a few salient points about the tool. First, the geometry generation code it contains is a bit cumbersome to use. Consequently, some of the less expensive commercial Computer-Aided Design/Computer-Aided Manufacture (CAD/CAM) packages are used to construct, convert, and repair configurations of interest. Second, the automated generation of Cartesian grids by the cubes component of Cart3D reduces the grid generation time to less than an hour for most cases. This attribute saves countless man-hours in problem setup time and greatly enhances productivity. Third, it has been found that the Cart3D geometry conversion programs work most successfully with the stereolithography (STL) solid model format produced by many CAD/CAM packages.

The enhancements made to TIGER by Robinson [3,4]: (1) permit the use of an algebraic enthalpy equation in lieu of the differential energy equation, (2) generalize the Runge-Kutta integration scheme [6] from its original four stages to "m" user-specified stages (usually two), (3) enhance robustness near flow corners and other high-gradient regions at high Mach numbers, and (4) add the vorticity confinement technique [7] to conserve field and surface-generated vorticity. These all serve to reduce computation time, increase reliability, and thereby enable the aerodynamicist to be more productive.

B. Application

Exploration of the helicopter jettison problem began with conversion of the missile and helicopter geometries into the STL format for use with ETA. The bulk of the missile geometry had been created in the process of designing and manufacturing a wind tunnel model of a very similar airframe, so it was quite detailed. It was produced in the form of an AutoCAD [8] three-dimensional assembly drawing along with parts drawings, all in the "AutoCAD drawing" (DWG) file format. Accordingly, AutoCAD was used to remove screw holes (the screws were missing from the model), internal test components, and the external leveling plate; create the appropriate nose section; and close the base. It was also used to convert the main body (consisting of all remaining components other than the tail flaps) and each tail flap into individual STL files that were successfully converted by and imported into ETA. The missile geometry (as imported into ETA) is shown in Figure 1. While this process was relatively straightforward, dealing with the helicopter geometry was much more difficult.

The helicopter model had its genesis as a detailed Catia [9] CAD geometry that was converted to an Initial Graphics Exchange Specification (IGES) format for subsequent use. Evidently, there were some conversion difficulties because the IGES files of the model components frequently had numerous disjointed and overlapping surface regions that should have been connected. However, none of these geometric disconnects were identified by the AutoCAD three-dimensional modeling tools (Inventor and Mechanical Desktop). Rather, the

Rhinoceros [10] (Rhino) Non-Uniform Rational B-Spline (NURBS) modeling software was required to identify the disconnects and repair the geometry.

It was found that the IGES files had to be imported into AutoCAD's Mechanical Desktop, converted to the 3D Studio (3DS) format, imported into Rhino, and examined for geometric disconnects. While the errors were visually identified in Rhino, the actual repairs were made on the 3DS file via Mechanical Desktop. It turned out that the errors were so numerous that partially mended files had to be iteratively passed between the programs. Upon completing the fixes, each file was checked for watertightness within Rhino, converted to the ACIS SAT format, exported to Mechanical Desktop, promoted to an AutoCAD "Part", exported to AutoCAD's Inventor as an SAT file, and then converted to an STL file. Although Rhino was able to create STL files, ETA was somehow unsuccessful in converting and importing them. ETA only seemed to accept Inventor's STL geometries. The final, converted, detailed helicopter geometry is shown in Figures 2 and 3.

After the very time consuming task of geometry repair and conversion was finished, ETA was exercised for the missile as it was jettisoned from the inboard launcher position of the helicopter (Fig. 4). Note that the launch rail is absent as it was unavailable at the time this study was initiated. The trajectory points at which computations were performed were selected from predictions made by a 6-DOF program—the same program requiring the results of this effort.

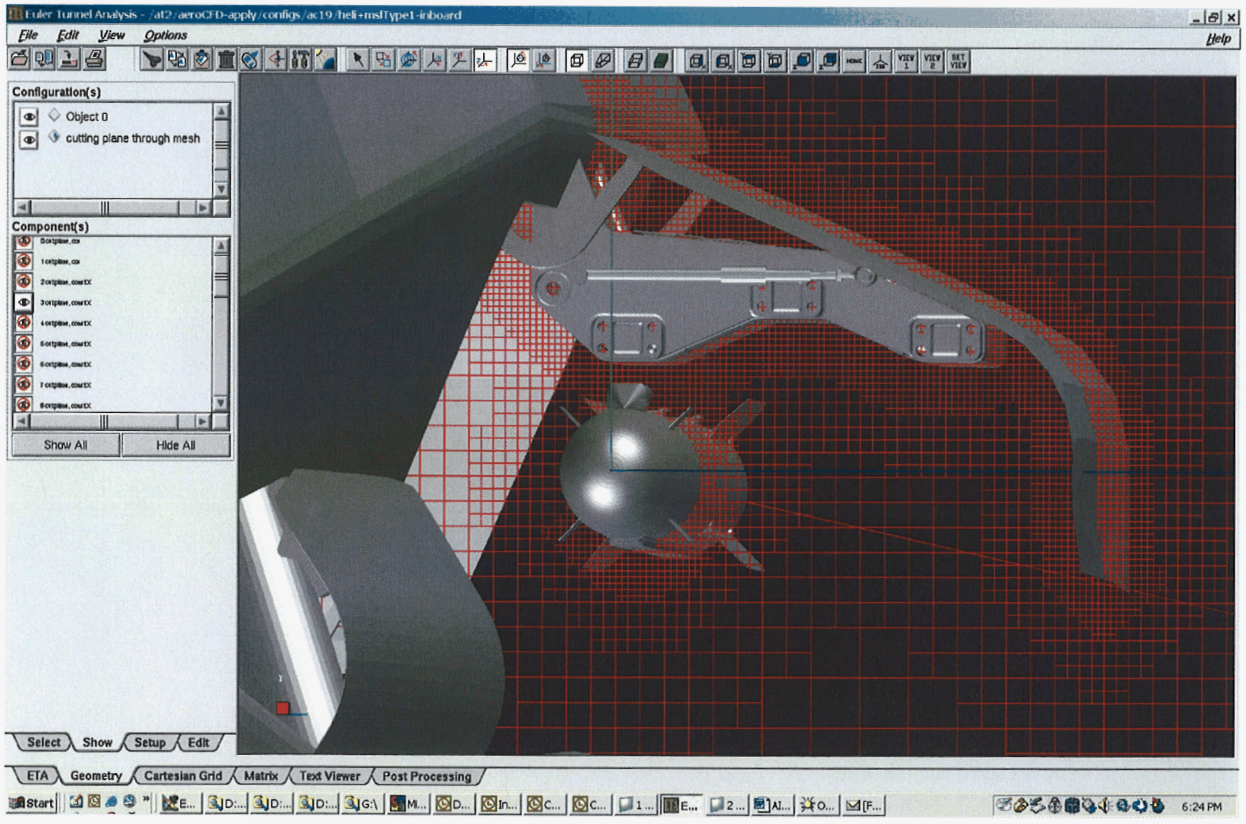

Figure 4. Close-Up of Missile at Inboard Launcher Position

Since it is most likely that an emergency jettison event would occur during forward flight, it was assumed that the velocity would be sufficient to convect the rotor downwash downstream of the region of interest. Although this assumption simplifies the problem, it is also consistent with the findings of Reference 11. For example, Figure 5 (adapted from this reference) shows measured results for a helicopter with a mid-body wing at a velocity of 120 knots. It can be clearly seen in the upper figure that flow vectors emanating from the rotor miss the wing region. In addition, the measured downwash angles (presented in the lower figure) are less than 10 degrees for speeds as low as 80 knots. While the helicopter of Figures 2 and 3 is a different airframe, its missiles are similarly located in the mid-body region and are likely to be unaffected at the same speeds. Further, the bay doors of this helicopter shield the missile from the rotor flowfield. Hence, it is quite tenable to neglect rotor downwash for this analysis.

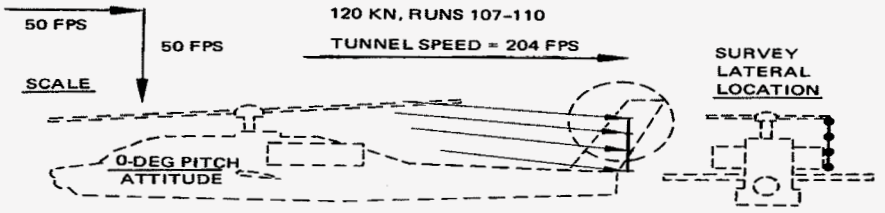

SYMB	RUN	TUNNEL SPEED, KN	α_f, DEG
○	70	40	2.5
□	71	50	1.9
△	72	60	1.1
▽	73	80	0.6
◇	74	100	0.5
◇	75	120	0.4

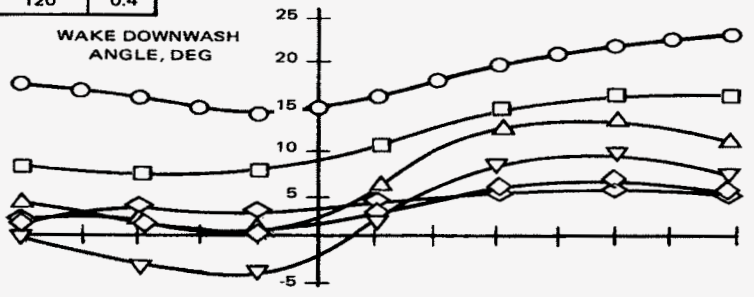

Figure 5. Flowfield Measurements for a Helicopter with a Mid-Body Wing

In order to ground the computations in reality, it was decided to calculate the force and moment coefficients of the isolated missile and compare them with wind tunnel measurements. Mach 0.5 (equating to a sea level speed of 331 knots) was the slowest available measurement condition for the missile. So computations were made for this condition even though it represents a faster speed than is achievable by most helicopters.

The initial calculations for the isolated missile placed it near the middle of the grid with outer boundaries located approximately eight missile body lengths from the center on all sides. Eleven levels of refinement were specified, but only one buffer cell was stipulated between each level. In addition, the imported model was comprised of five components: the

main missile and four movable tail flaps. While the missile-alone coefficients exhibited the same general trends as the data, the agreement was not as good as desired. Further, when subsequent computations were made in the presence of the helicopter, the predicted proximity effects were too extreme to be believed. This was observed at all positions so it was suspected that some sort of error was occurring consistently.

In examining the methodology, it appeared that the helicopter model, imported as 27 individual components, was "pushing the limit" of TIGER's bookkeeping arrays. Perhaps more importantly, though, the outer bounds of the grids were located very close to the bodies (that is, roughly 1.5 helicopter body lengths from the fuselage in each direction), with eleven levels of refinement and one buffer cell. It was understood at the time that such a small domain size was inadequate for subsonic computations, but the interest then was only to perform an initial, preliminary assessment within a very short timeframe. There was not sufficient time to maximize the domain size while keeping the number of grid cells small enough to fit within the available computer memory.

Since that time, such an assessment has been made with its results being used to size the domains for the current effort. In addition, the individual helicopter and missile parts were concatenated to produce single-component geometries to avoid bookkeeping trouble. Further, the isolated missile calculations were performed with the helicopter simultaneously resident in the grid but located too far away to produce any noticeable influence. This was likewise done to circumvent any spurious bookkeeping trouble. The resulting grid located the missile 5,000 inches directly below the inboard jettison position, placed the origin of the coordinate system on the tip of the missile nose, positioned the grid boundaries at least about 28 helicopter body lengths away from the origin on all sides, applied 15 levels of refinement, and specified 4 buffer cells. This arrangement (Figs. 6 and 7) created approximately 4.8 million grid cells and fit well within the available computer memory. The smallest cells lay adjacent to the body with a longitudinal dimension about seven thousandths (7/1000) of the missile body length, and lateral dimensions around four thousandths (4/1000) of the length.

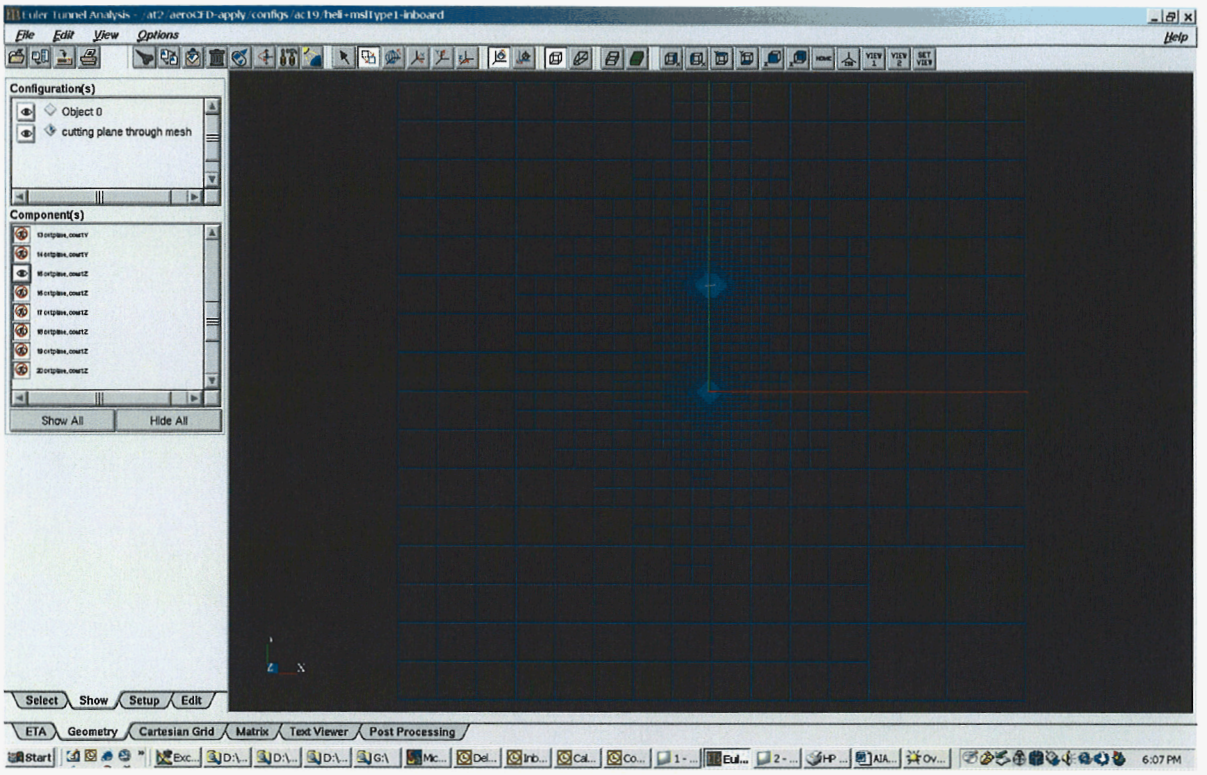

Figure 6. Configuration Geometry and Grid Used for Isolated Missile Computations

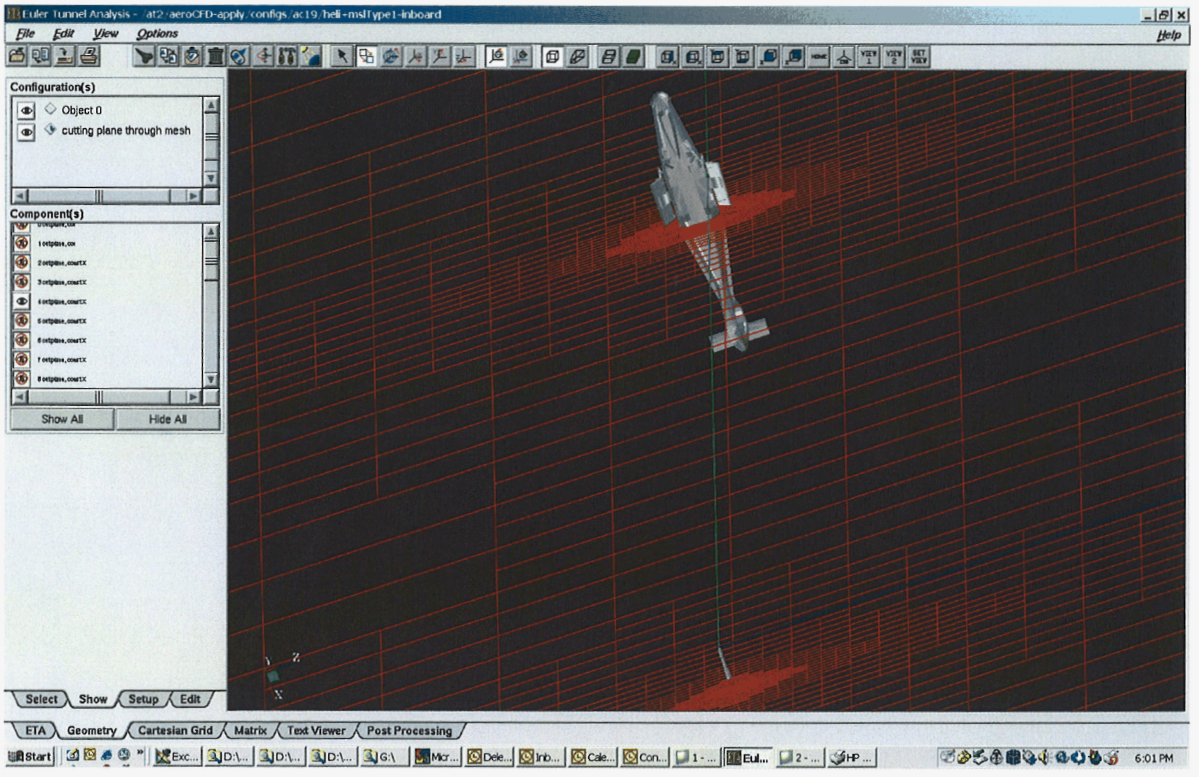

Figure 7. Close-Up of Geometry and Grid Used for Isolated Missile Computations

The parameters just described were used to construct all of the grids for this investigation while, as previously mentioned, predicted trajectory points were provided by the 6-DOF program needing the results of this effort. The selected points were located 0 inches (pre-jettison), 6 inches, 57 inches, and 105 inches below the carriage position.

The first point was clearly expected to experience significant viscous phenomena. However, it was hoped that the TIGER Euler solver of ETA would be able to capture the relevant rotational effects and provide a reasonable estimate of influence effects until sufficient time and funding for viscous computations became available. The 105-inch point was selected based on an intuitive estimate of where the missile would experience freestream flow. The intermediate jettison positions were picked at approximately 5 percent and 50 percent of the distance between the initial and last locations.

As previously stated, flowfields and aerodynamic coefficients were computed (with vorticity confinement) for a Mach number of 0.5 to compare with measurement. The angle of attack was varied from –4 degrees to +20 degrees (with intermediate values of +0, +4, +6, +10, +12 and +16 degrees) to construct coefficient versus angle-of-attack comparisons with wind tunnel data. The angle of attack of both the helicopter and missile were varied simultaneously at the carriage and "freestream" locations. However, the helicopter was maintained at a zero-degree attitude while the missile angle was varied at the intermediate positions. It should be noted that although the 6-DOF predicted additional missile body rotation angles at each point, these were all set to zero to enhance understanding of the results and provide common points of reference.

III. RESULTS AND DISCUSSION

Results from the initial calculations are shown in Figures 8 through 11. In these graphs, it can clearly be seen that while the isolated missile normal force and pitching moment curves (Figs. 8 and 9) exhibit the general trends of the measured data, the actual agreement is not particularly good. Further, the jettisoned-missile normal force curves in Figure 10 indicate that the helicopter negates lift for all angles of attack at all locations—an unbelievable result. Similarly, the jettisoned-missile pitching moment plot of Figure 11 shows the missile experiencing little change in moment at any position—another unlikely result, especially for locations at or near the helicopter. These incredible comparisons prompted the subsequent set of computations as previously described. For clarity, the jettison positions that were studied are presented in Figure 12 while the results are shown in Figures 13 through 18.

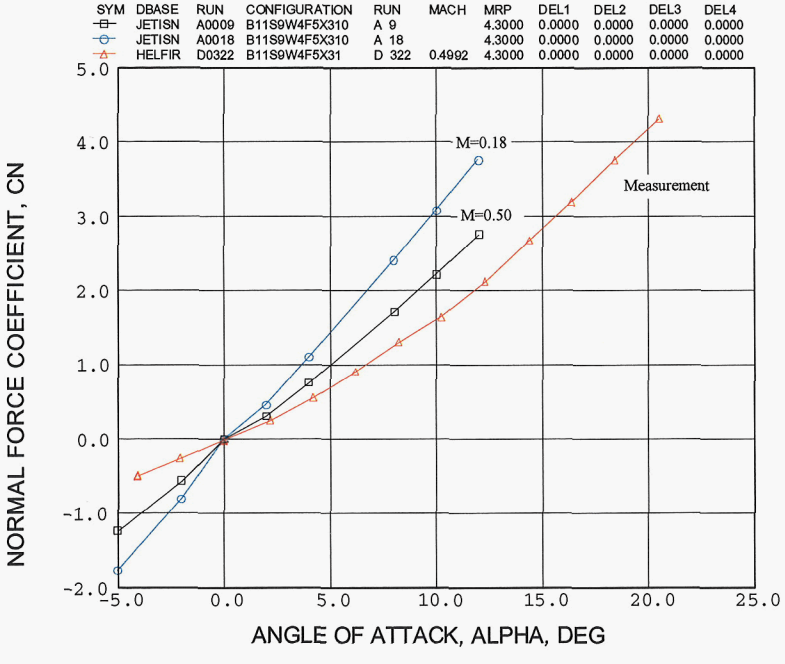

Figure 8. Initial Normal Force Curve for Isolated Missile

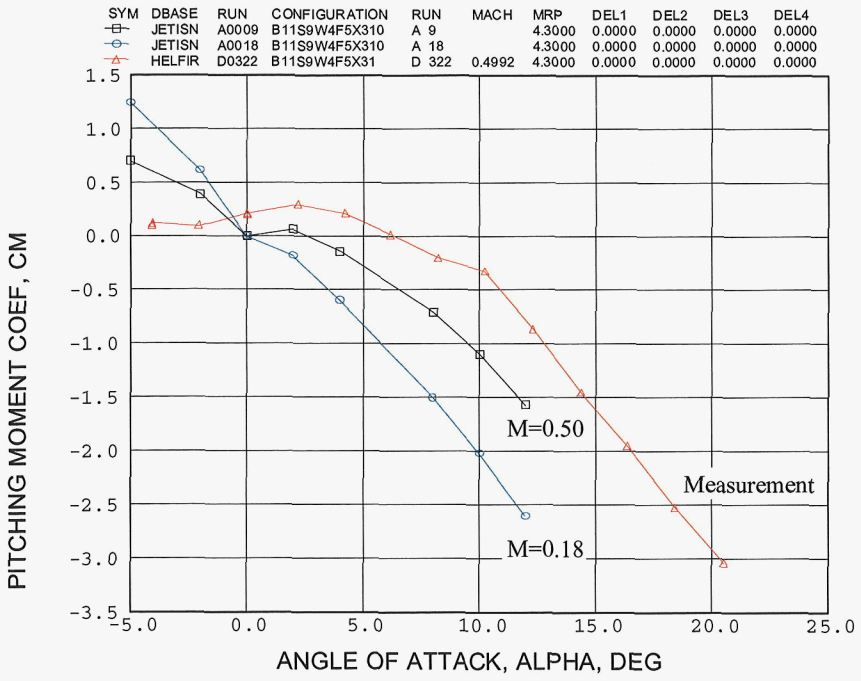

Figure 9. Initial Pitching Moment Curve for Isolated Missile

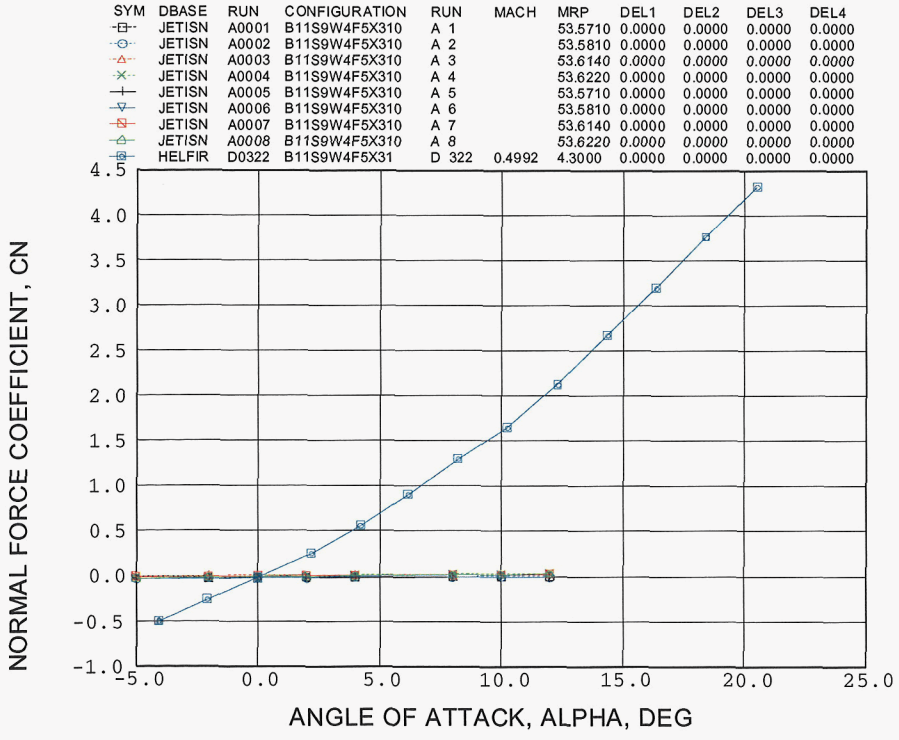

Figure 10. Initial Normal Force Comparison of Missile in the Presence of the Helicopter

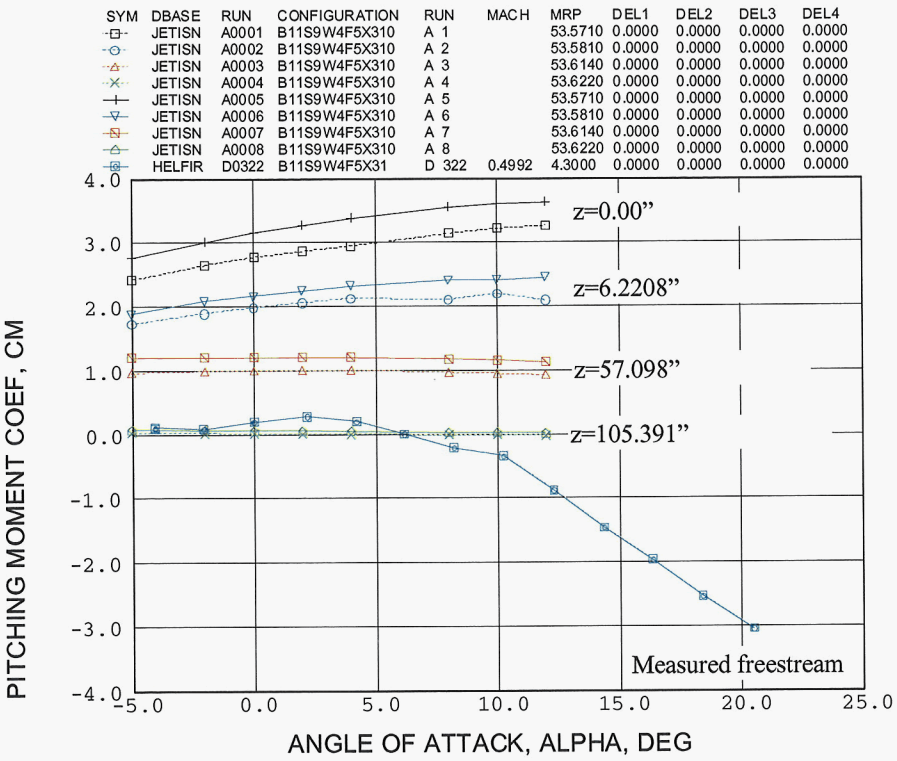

Figure 11. Initial Pitching Moment Comparison of Missile in the Presence of the Helicopter

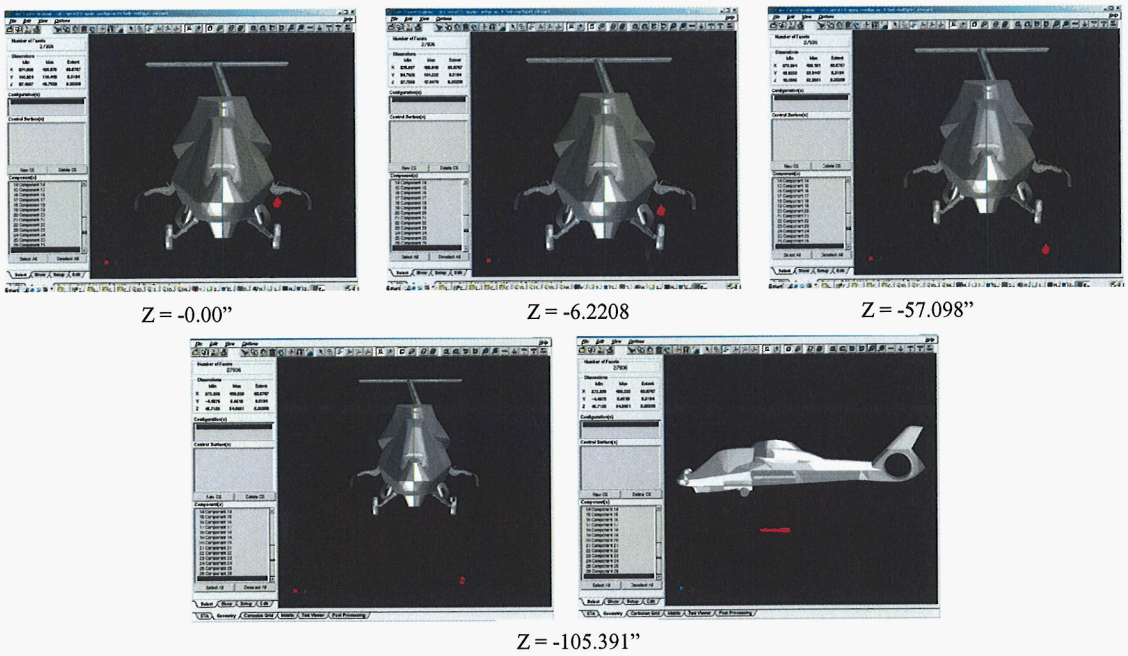

Figure 12. Jettison Positions of Missile with Respect to Helicopter

Figure 13 presents the normal force coefficient versus angle of attack for all cases. It can be seen that the agreement between the freestream computation and measurement is much better than for the initial calculations. It can also be seen that the helicopter fuselage not only decreases but in fact changes the direction of the normal force at the pre-jettison position. However, this effect is reduced appreciably at the 6-inch location such that the slope of the curve is again positive. The fuselage effect continues, however, such that at the 57-inch and 105-inch stations the slope and magnitude of the normal force curve is increased significantly beyond that of the "freestream" missile.

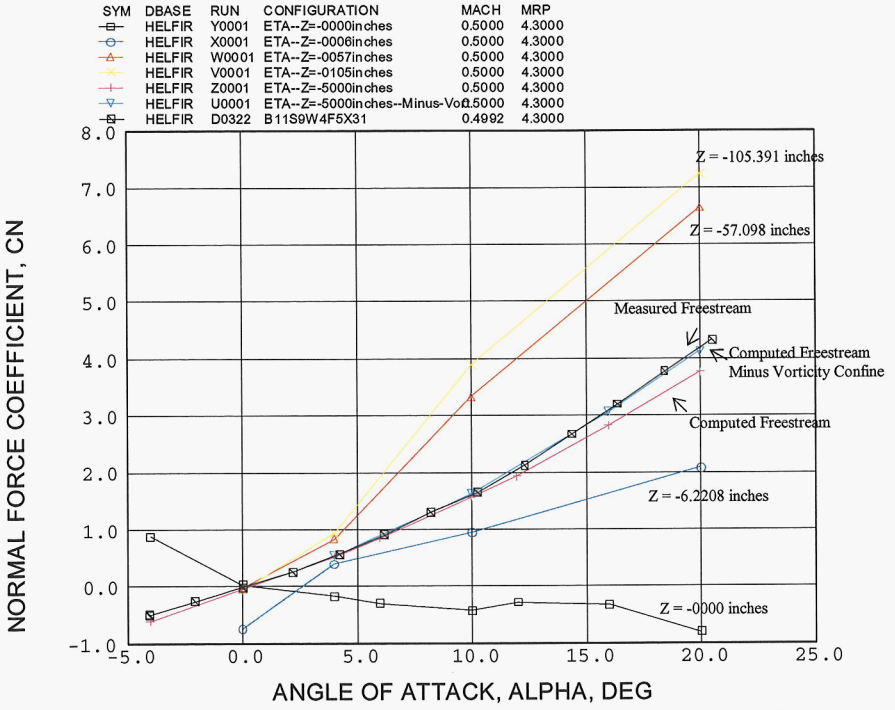

Figure 13. Normal Force of Missile in the Presence of the Helicopter

Figure 14 shows the comparisons for pitching moment about the mid-body of the missile—a comparison that amplifies any differences. In this plot, it is found that the agreement between the freestream computations and wind tunnel data is quite good. The freestream computations produce the region of neutral stability (between -4 and about +10 degrees) where vortices from the strakes influence the flow around the tail fins. In addition, the freestream calculations also capture the change in slope that occurs above +10 degrees, although not as crisply as desired. Regardless, the fact that these phenomena are correctly portrayed by ETA testifies to vorticity confinement's conservation of strake-generated vorticity as it convects downstream to the tail fins. The effect of the fuselage is quite pronounced in that it makes the missile completely unstable at the carriage position. However, this influence is reversed at the 6-inch location such that the missile behaves much more like it would in a freestream. At the 57-inch and 105-inch positions, the behavior becomes much like that of a missile in freestream flow except that the abrupt change in slope occurs much sooner at +4 degrees angle of attack. The disappearance of the neutral stability region at the pre-jettison position indicates that the fuselage interferes significantly with this interaction. However, the fact that neutral stability returns at subsequent

drop distances indicates not only the reconstruction of the interaction, but also that it is strong enough to produce an observable outcome even at the 6-inch position.

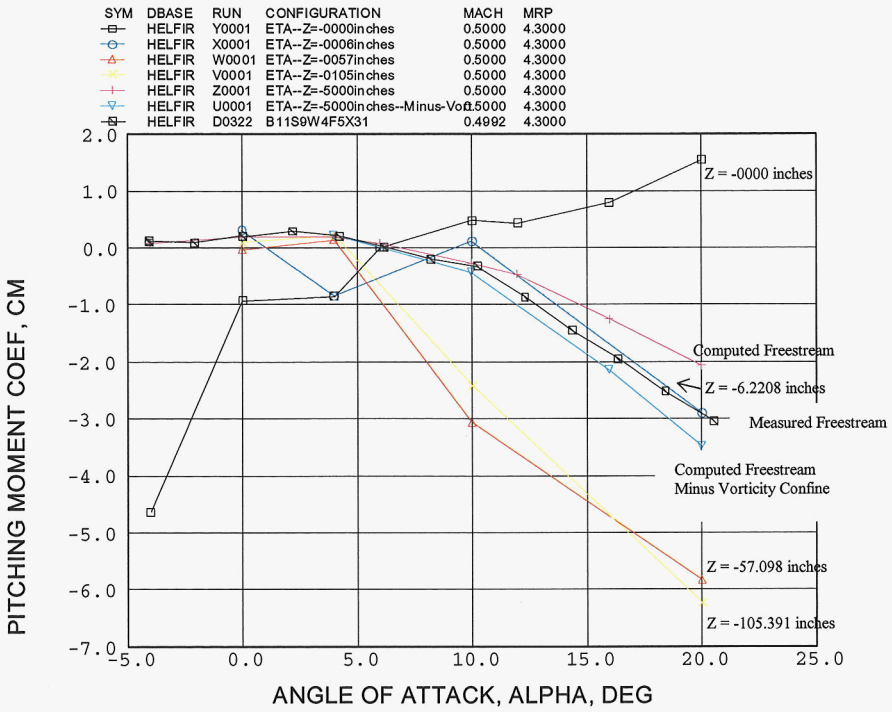

Figure 14. Pitching Moment of Missile in the Presence of the Helicopter

The side force coefficient, shown in Figure 15, is observed to be essentially zero in both the measurement and freestream calculations. At the pre-jettison site, though, the helicopter fuselage exhibits a very large influence and pushes the missile in the outboard direction. The magnitude of this effect is on the order of the freestream normal force and is much larger than was anticipated. Nevertheless it behaves as intuition would indicate and diminishes with increased vertical distance, approaching the freestream value of zero. The resulting yawing moment coefficient is presented in Figure 16. While this moment decreases with drop distance, like the side force, it has a magnitude at the 0-inch and 6-inch locations that is much greater than the freestream pitching moment. In fact, at these positions, the missile will yaw towards the helicopter even more quickly than it will go unstable in pitch. This is a serious condition that must be accounted for in jettison simulations.

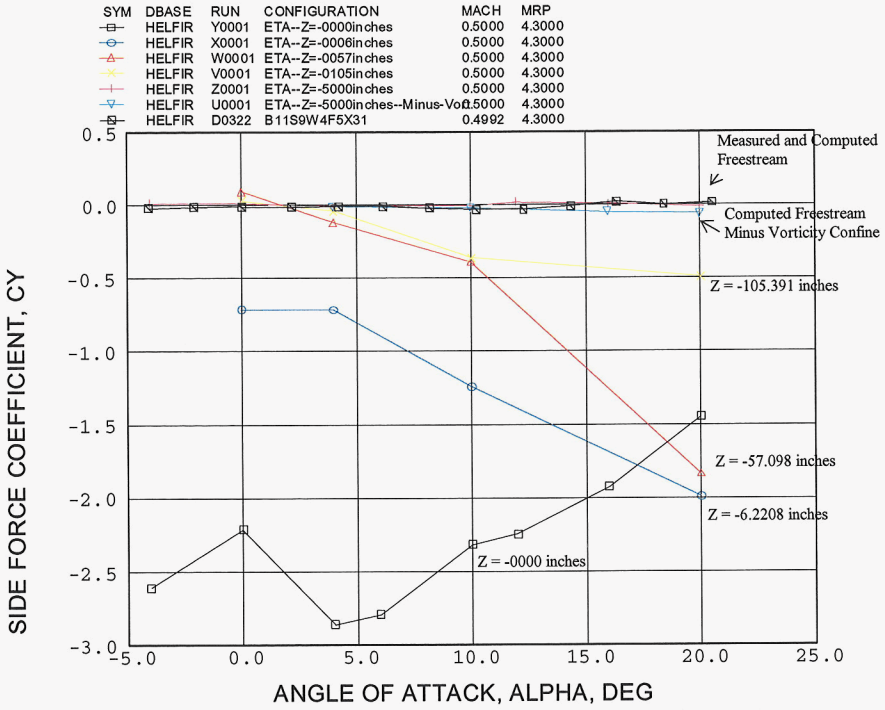

Figure 15. Side Force of Missile in the Presence of the Helicopter

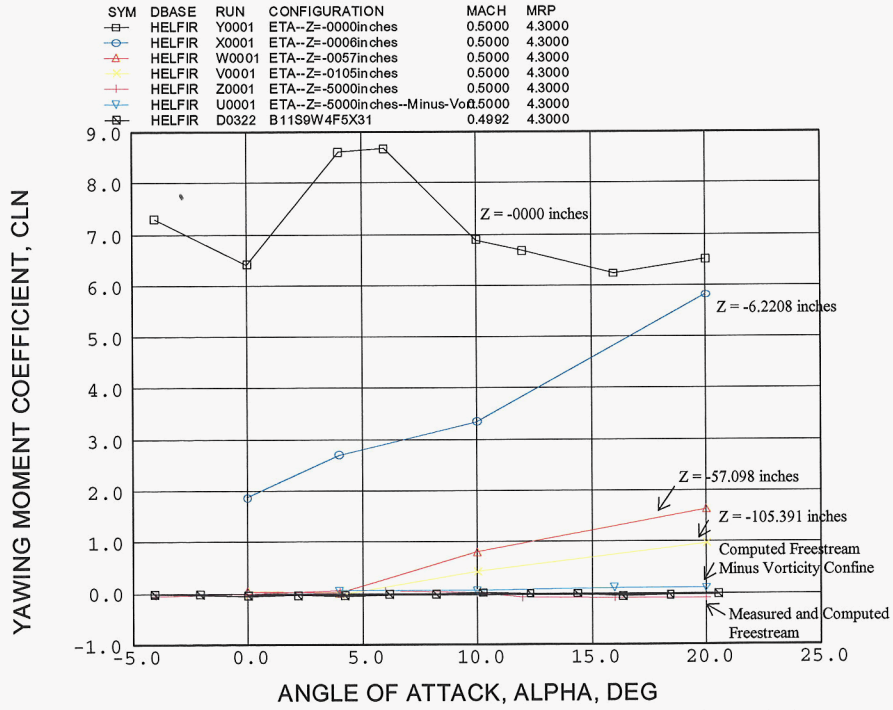

Figure 16. Yawing Moment of Missile in the Presence of the Helicopter

In Figure 17, it is evident that the rolling moment starts out relatively small at the carriage position and varies from negative (below about 2 degrees) to mostly positive, rolling toward the fuselage, above 2 degrees angle of attack. At 6 inches, however, it increases greatly with angle of attack. Then the moment decreases with distance and approaches the freestream value of zero.

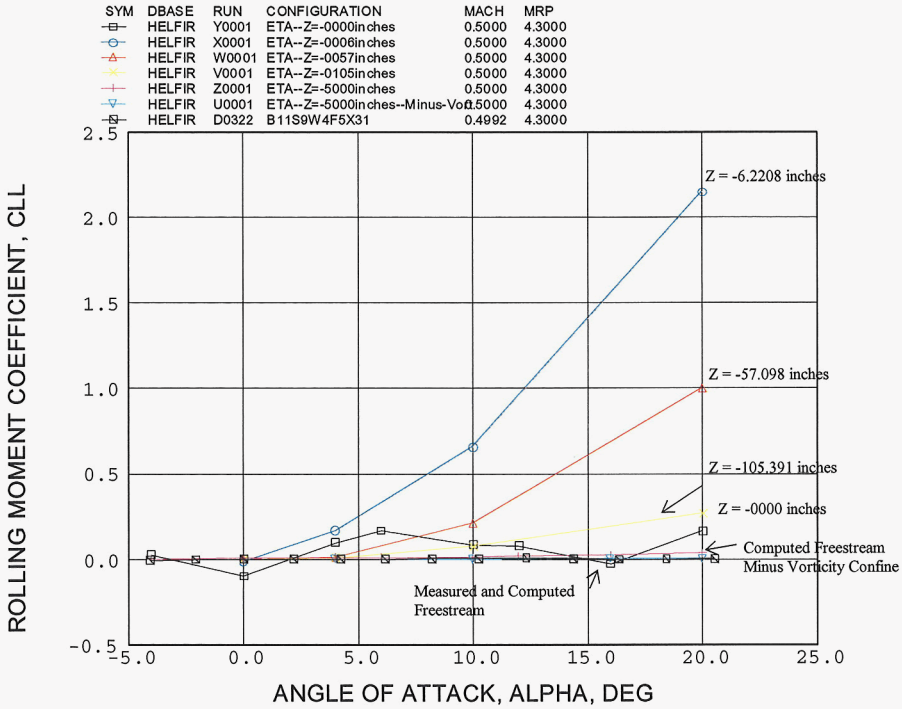

Figure 17. Rolling Moment of Missile in the Presence of the Helicopter

The effect of the helicopter on axial force is presented in Figure 18. Although the predicted axial force is only that of an inviscid Euler code utilizing vorticity confinement, the computation is seen to agree reasonably with the freestream measurements. It is also found that while the fuselage essentially increments the missile drag at the pre-jettison station, it causes a much more drastic increase with angle of attack (above 5 degrees) as drop distance increases. This is likely due to the flowfield induced by the helicopter fuselage at these stations. And it is consistent with the large slope in the normal force curve (Fig. 13) at the 57-inch and 105-inch spots, as well as the combined magnitude of the normal and side forces at the 6-inch location.

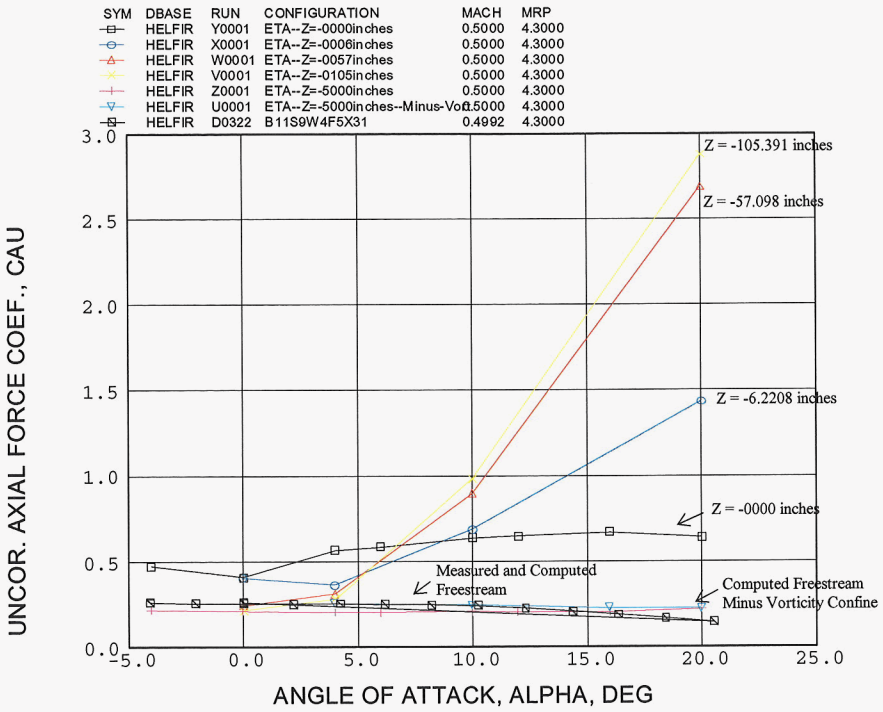

Figure 18. Axial Force of Missile in the Presence of the Helicopter

While all the previously discussed computational results were obtained using vorticity confinement, it was decided to examine the consequence of omitting this feature. The resulting curves are simultaneously provided in Figures 13 through 18. In examining the normal force and pitching moment plots, Figures 13 and 14, it was surprising to find that the computations without vorticity confinement matched the freestream measurements more closely than those with this feature. The "without" normal force curve is indistinguishable from the data, and the corresponding pitching moment graph captures the abrupt change in moment (at +10 degrees) very well. Both sets of calculation used the same grids, but this may be an issue of convergence. The vorticity confinement method requires the use of the full energy equation during its solution process, while calculations without the method can use an algebraic total energy equation. Hence, more iterations can be accomplished without vorticity confinement within the same amount of CPU time. Nevertheless, the result is quite interesting and merits more detailed investigation.

IV. SUMMARY

The ETA methodology has been applied to assess the effect of a nearby helicopter fuselage (omitting rotor downwash) on the aerodynamic properties of a jettisoned missile with forward strakes. Initial computations performed with a small computational domain indicated a striking but unbelievable effect. However, subsequent calculations made with a much larger domain showed (1) very good comparisons with freestream wind tunnel measurements, and (2) much more reasonable but still striking effects on the missile's aerodynamic properties. All properties were impacted but the pitching and yawing moments were the most drastically altered (compared to freestream) at and near the helicopter. These moments indicated a propensity to yaw into the helicopter while going unstable in pitch. It is recognized that in many cases missiles are jettisoned enmasse with the launcher during an emergency. And in such cases tip-off, inertia, and gravity will likely be the dominating phenomena. However, if flight speeds are fast enough or if missiles are to be jettisoned individually, aerodynamic forces and moment can become large enough to be of importance. In these instances, the non-freestream behavior of the missile in the presence of the helicopter is essential to incorporate into a jettison trajectory simulation, particularly when examining issues of pilot safety. In short, if the aerodynamic properties of the missile are important at all, the use of freestream properties is inadequate and should be replaced with aerodynamic characteristics in the presence of the fuselage.

REFERENCES

1. Aftosmis, M. J., Berger, M. J., and Melton, J. E., "Robust and Efficient Cartesian Mesh Generation for Component-Based Geometry," AIAA Paper 97-0196, Jan. 1997; and AIAA Journal, Vol. 36, pp, 952-960, June 1998.

2. Melton, J. E, Berger, M. J., and Aftosmis M. J., "3D Applications of a Cartesian Grid Euler Method," AIAA Paper 95-0853, July 1995.

3. Robinson, M. A., "SY-TIGER code Version 5.9 Release Notes & Guide," SYColeman Memorandum, 01 October 2003.

4. Robinson, M. A., "Application of Vorticity Confinement to Inviscid Missile Force and Moment Prediction," AIAA Paper 2004-0717, January 2004.

5. Vaughn, M. E., Jr. and Auman, L. M., "Assessment of a Productivity-Oriented CFD Methodology for Designing a Hypervelocity Missile," AIAA Paper 2003-3937, June 2003.

6. Jameson, A., Schmidt W., and Turkel, E., "Numerical Solutions of the Euler Equations by Finite Volume Methods Using Runge-Kutta Time-Stepping Schemes," AIAA Paper 81-1259, June 1981.

7. Dietz, W., Fan, M., Steinhoff, J., and Wenren, Y, "Application of Vorticity Confinement to the Prediction of the Flow Over Complex Bodies – A Survey of Recent Results," AIAA Paper 2001-2642, June 2001.

8. Autodesk Inventor Series 5, Getting Started, Autodesk, Inc, December 2001.

9. http://plm.3ds.com/10+M52c1d207f79.0.html

10. Rhinoceros NURBS Modeling for Windows, Version 3, User's Guide, Robert McNeel & Associates, 2002.

11. Logan, A. H., Prouty, R. W., and Clark, D. R., "Wind Tunel Tests of Large- and Small-Scale Rotor Hubs and Pylons," USAAVRADCOM-TR-80-D-21, April 1981.

INITIAL DISTRIBUTION LIST

		Copies
Weapon Systems Technology Information Analysis Center Alion Science and Technology 201 Mill Street Rome NY 13440	Mr. Perry Onderdonk ponderdonk@alionscience.com	Electronic
Defense Technical Information Center 8725 John J. Kingman Rd., Suite 0944 Fort Belvoir, VA 22060-6218	Jack Rike jrike@dtic.mil	Electronic
AMSRD-AMR	Dr. William McCorkle Bill.McCorkle@us.army.mil	Electronic
AMSRD-AMR-CS-IC		Electronic
AMSRD-AMR-SS,	Gregory B. Tackett Gregory.Tackett@us.army.mil	Electronic
AMSRD-AMR-SS-AT,	Lamar M. Auman lamar.auman@us.army.mil	Electronic
	Milton E. Vaughn, Jr. Ed.Vaughn@us.army.mil	Electronic
AMSRD-L-G-I,	Ms. Anne Lanteigne anne.lanteigne@us.army.mil	Electronic